Appl Compos Mater (2012) 19:443–458
DOI 10.1007/s10443-011-9217-8

Compaction Behavior and Part Thickness Variation in Vacuum Infusion Molding Process

Jinshui Yang · Jiayu Xiao · Jingcheng Zeng · Dazhi Jiang · Chaoyi Peng

Received: 6 May 2011 / Accepted: 22 June 2011 / Published online: 8 July 2011

Abstract In vacuum infusion molding process (VIMP), it is difficult to manufacture a composite part with small dimensional tolerance, since the upper mold for the process is flexible. In this study, the static and cyclic compaction responses of five kinds of fabrics were experimentally studied under real VIMP conditions, with the effects of compaction pressure, compaction time, compaction cycle and number of the fabric layers. The static and cyclic compaction responses of the all fabrics follow different power law models and the resulting fiber volume fraction and relaxation factor increase with the number of layers. Although the resulting fiber volume fraction increases with the layer numbers, change of the fiber volume fraction of the composite parts with 10 layers to 100 layers of the all fabrics is less than 2.5%. The thickness of the composite part was monitored and measured using micrometer gauges, and the effects of processing parameters on the final thickness of part was investigated. The part thickness varies as a function of spatial coordinates and time during pre-filling, filling and post-filling stages in VIMP. The variation and the final value of the part thickness would be significantly affected by the processing parameters. Statistical results show that the final part thickness is equivalent to the thickness of the dry preform under the 0.08 MPa vacuum compaction pressure in VIMP. The difference between the fiber volume fraction of the final part and that of the dry preform is 2%~5.7%.

Keywords Vacuum infusion molding process (VIMP) · Compaction behavior · Composite materials · Fiber volume fraction · Thickness · Fabric preform

1 Introduction

Vacuum infusion molding process (VIMP) is a closed mold composite manufacturing process in which only one side of the mold is solid. A flexible vacuum bag is used as the other side of the mold to close the mold cavity. A vacuum is applied to compact the reinforcement material

J. Yang (✉) · J. Xiao (✉) · J. Zeng · D. Jiang · C. Peng
College of Aerospace and Material Engineering, National University of Defense Technology, Changsha, China 410073
e-mail: xjtujinshui@yahoo.com.cn
e-mail: jiayuxiao@tom.com

and to drive the resin through the porous fabric preform [1, 2]. VIMP is widely used to manufacture large scale composite structures, such as wind turbine blades, pressure vessels, panels for boats, etc. The VIMP can be divided into four process stages [3, 4]:lay-up, pre-filling, filling and post-filling. In the lay-up stage, fabric preform is laid on the solid side of the mold. A layer of peel-ply is generally laid over the preform, allowing for easy separation of the part from the consumables (include vacuum bag, distribution medium, resin and vacuum tubes, etc.). Distribution medium can be over the peel-ply to enhance resin flow. Once resin inlet and vacuum vent tubes are in place, the mold is closed using a vacuum bag sealed with sealant tape. With the cavity sealed, the inlet is clamped and vacuum is applied to compact the preform, this stage being referred to here as the "pre-filling" stage. At the end of pre-filling stage, the inlet is opened and the resin penetrates the preform. During this "filling" stage, pressure inside the cavity varies in position and time. Once the resin flow front reaches the end of the preform, the inlet is usually clamped, stopping flow of resin into the cavity. This "post-filling" stage involves removal of excess resin, and allows resin pressure and laminate thickness to equilibrate within the cavity. Once the resin is fully cured, the vacuum is released and the part is lifted off the mold and separated from the consumables. The setup and different process stages of VIMP is shown in Fig. 1.

The most important drawback of VIMP for producing large scale structures is thickness variation of the part due to non-uniform compaction pressure. As the compaction pressure

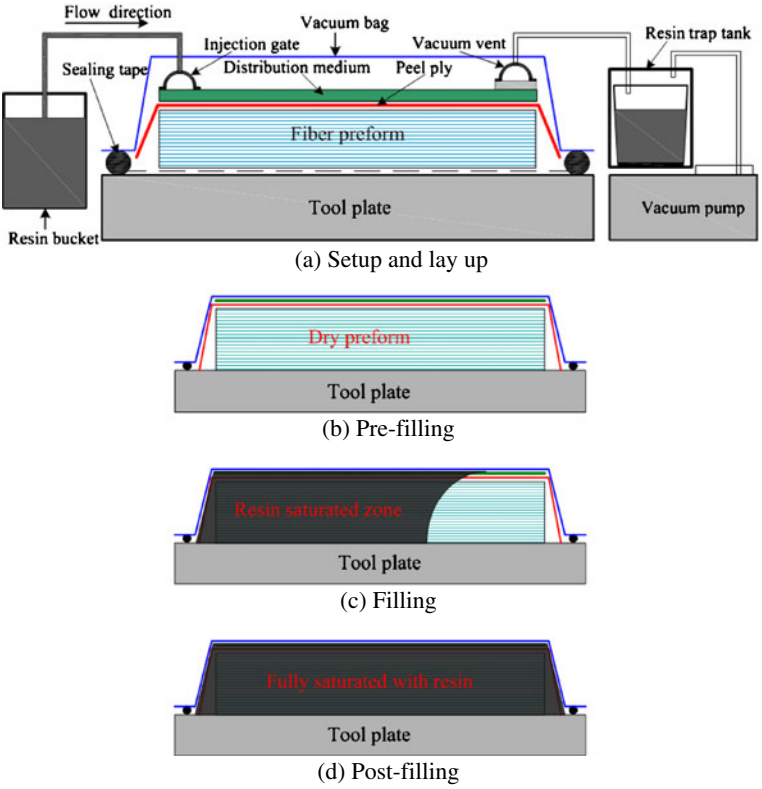

Fig. 1 Setup and different process stages of vacuum infusion molding process. **a** Setup and lay up, **b** Pre-filling, **c** Filling, **d** Post-filling

on the vacuum bag decreases due to an increase in the resin pressure, the part thickness varies as a function of spatial coordinates and time [5]. Even after the injection is completed, the part thickness might still vary due to the compacted preform relaxation, resin redistribution and resin shrinkage during post-filling and curing stage. Many researchers have investigated the VIMP with experiments and models to understand the physics of the process, and thus to overcome the issues. Kelly et al. [6] and Hammami et al. [7] performed compaction and relaxation experiments on different kinds of fabric preforms. They observed that the compression and relaxation characteristics depend both on the structure of the fabric, and on whether the fabric is dry or wet. Luo et al. [8] and Robitaille et al. [9] used a power law to fit their experimental compaction data. Luo et al. [8] modeled the relaxation of the fabric by using the dissipated energy method. Yenilmez et al. [5] performed compaction experiments to identify the relationship between fiber volume fraction and compaction pressure. In the previous work, a hard steel block was chosen to provide compaction load to simulate the vacuum pressure conditions in VIMP. The loading way cannot simulate the fabric preform relaxation in the VIMP. In order to simulate the real condition better in VIMP, the compaction tests were conducted under the real vacuum pressure condition to study the compaction behavior of the fabrics in this paper.

Tackitt et al. [10] used linear variable differential transducers to measure the thickness of the fabric preform during resin infusion. In the infusion experiment, further fiber nesting occurred near the flow front, and fabric preform became more compacted. This phenomenon was explained by the lubrication effect [7]. After the flow front passed the nested section, thickness of the fabric preform started to increase. Yenilmez et al. [5] monitored the thickness and resin pressure using multiple dial gages and pressure transducers during resin filling stage in VIMP. And the results were compared with the model developed by Correia et al. [11]. But the thickness variation of the fabric preform during post-filling and curing stage has not been characterized in previous literature. The rule of the part thickness variation during pre-filling, filling and post-filling stages was investigated in this paper.

VIMP is generally used for large scale parts, faulty production results in high expense. To achieve a desired thickness in the final product, one should model the coupled fabric compaction and resin flow. By using the model, the thickness distribution of the final part can be estimated; the fabric and injection gate configuration can be tailored to achieve the desired thickness. Additionally, the mold filling time can be calculated, and thus curing time can be optimized to shorten the cycle time. The final thickness of the part, which can be expressed by the fiber volume fraction (V_f) equivalently, is governed by the compaction behavior of the fabric preform as well as the vacuum pressure [7].

The first objective of this study is to characterize the compaction behavior of fabric preform under the vacuum pressure. Effects of vacuum, load time, repeated compaction cycle and number of layers were investigated. The second objective is to characterize the thickness variation of fabric preform during pre-filling, filling and post-filling stages in VIMP. Such information will be useful in predicting the final part thickness and modeling resin flow in VIMP.

2 Materials and Experimental Procedure

2.1 Materials

Five kinds of fabrics, used as reinforcement materials in wind turbine blade, are illuminated in Table 1 and tested in the present work. The carbon fabric was procured from the Toray

Table 1 Properties of fabrics

Fabric	Specification	Fiber	Type	Superficial density/g·m^{-2}
300CUD	CFF-I-300	T700 carbon	Unidirectional	300
600GUD	EKU600(0)	E-glass	Unidirectional	600
1250GUD	EKU1150(0)/50E-120	E-glass	Unidirectional	1250
1215GTD	EKT1200(90,±45)E-1270	E-glass	Tri-axial knitted	1215
808GDD	EKB800(45,-45)E-1270	E-glass	Bi-axial knitted	808

Group in Japan, and the glass fabrics were provided by Chongqing Polycomp International Corp. in China. Photographs of fabrics are shown in Fig. 2.

An epoxy infusion resin, RIMR135/RIMH137 by Hexion Specialty Chemicals was used in the experiments. RIMR135 is resin and RIMH137 is additive. Density, viscosity and gelation time of RIMR135/RIMH137 at room temperature (~25°C) are tabulated in Table 2.

2.2 Compaction Procedure

The compaction tests were conducted under vacuum pressure. Figure 3 shows the schematic of compaction experimental setup. The pressure applied on the film was controlled by a vacuum pump. The changes of thickness were measured by a micrometer gauge. Since the surface of the fabric is irregular, small lightweight square plate is placed under the tips of dial gauges to measure an averaged thickness at gauge locations.

Compaction tests could be divided into three parts: step compaction, successive compaction and cyclic compaction. The step compaction is to investigate the influence of vacuum pressure on the compaction behavior in VIMP. During the step compaction test, a set of step compaction pressure, increasing from 0.00 MPa to 0.10 MPa with an interval of 0.01 MPa were applied. For taking account of relaxation in the fibers of the preform under a given vacuum pressure, the thickness of the specimen was registered after the compaction pressure became stable for 5 min. The compaction pressure is 0.10 MPa in the successive compaction test process, and the thickness was recorded in an interval of every 5 min for at least 1 h. And during cyclic compaction test, a cyclic pressure, increasing from 0.00 MPa to 0.10 MPa was applied, and then it was decreased back to the starting value. In cyclic compaction test process, the thickness of the sample was registered if it did not change in 2 min after the vacuum pressure became stable.

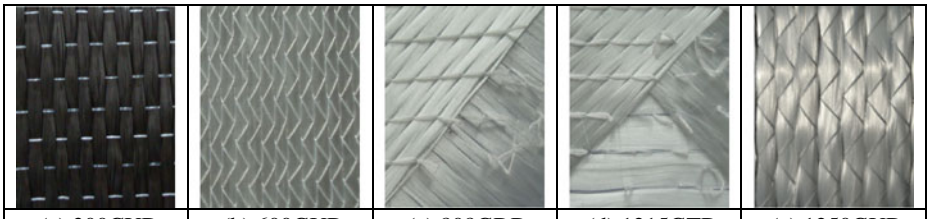

(a) 300CUD (b) 600GUD (c) 808GDD (d) 1215GTD (e) 1250GUD

Fig. 2 Photographs of various fabrics. **a** 300CUD, **b** 600GUD, **c** 808GDD, **d** 1215GTD, **e** 1250GUD

Table 2 Epoxy infusion resin RIMR135/RIMH137 properties at room temperature (~25°C)

RIMR135/RIMH137 mass ratio	Density/g·cm^{-3}	Viscosity/mPa·s	Gelation time/min	Supplier
100:30±2	1.08–1.12	200–300	250–260	Hexion Specialty Chemicals

2.3 Fiber Volume Fraction and Relaxation Factor

Fiber volume fraction V_f can be calculated by:

$$V_f = \frac{\rho_a n}{\rho h} \tag{1}$$

Where n is the number of layers, ρ_a is the superficial density of the fabric, ρ is the density of the fiber (carbon=1800 g/m^3, fiberglass=2540 g/m^3), and h is the thickness of specimen under compaction.

The relaxation factor R is defined as [3]:

$$R = \frac{h_i - h_f}{h_i} \tag{2}$$

Where h_i is the initial thickness, h_f is the final thickness after compaction pressure became stable at least 5 min. The higher the relaxation factor, the more relaxation occurs.

3 Results and Discussion

3.1 Effect of Vacuum Pressure

It was suggested that the compaction response of fabrics can be expressed by a two-parameter power law model representing the fiber volume fraction as a function of the compaction pressure [12, 13]:

$$V_f = a \cdot P^b \tag{3}$$

Where P is the compaction pressure, a and b are the experimental parameters dependent on the reinforcement used. In this paper, regression analysis was conducted to fit the experimental compaction results to the two-parameter power law model shown as Eq. 3. Fitting results show that there is a large deviation between the two-parameter power law model fitting results and the experimental data, and the best fit of data can be obtained by using the following three-parameter power law model Eq. 4, as shown in Fig. 4(a). Good

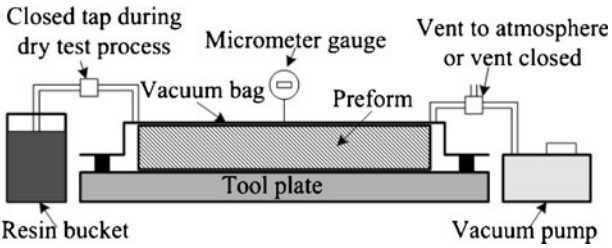

Fig. 3 Schematic of compaction experimental setup

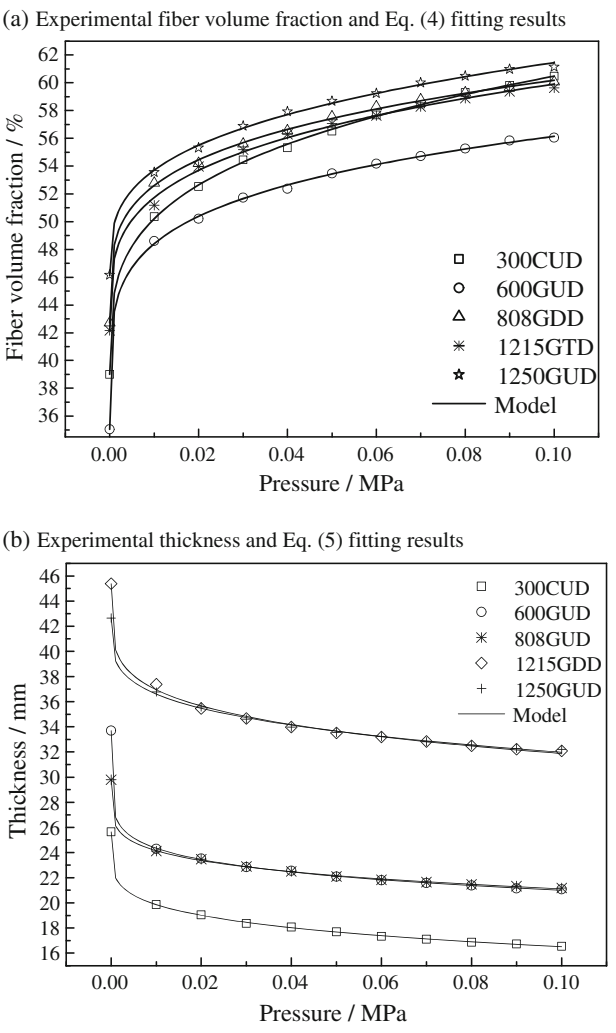

Fig. 4 Compaction behavior of five fabrics under the step vacuum pressure. **a** Experimental fiber volume fraction and Eq. 4 fitting results, **b** Experimental thickness and Eq. 5 fitting results

agreement was observed between the five sets of experimental data and the three-parameter power law model fit.

$$V_{\mathrm{f}} = a \cdot P^{b} + V_0 \tag{4}$$

Where V_0 is referred to the initial fiber volume fraction under 0.00 MPa vacuum compaction pressure. It should be noted that the corresponding relationship between the fabric preform thickness and the compaction pressure can be expressed with the following model:

$$h = h_0 - c \cdot P^{d} \tag{5}$$

Where h is the thickness of the preform under compaction pressure P and h_0 is the thickness of the preform at P=0.00 MPa, c and d are the experimental parameters. Eq. 5 fitting results and the experimental data are shown in Fig. 4(b). The parameters obtained are listed in Table 3.

Table 3 Fitted parameters for compaction pressure models

Fabric	a	b	V_0/%	h_0/mm	c	d
300CUD	41.12	0.2823	39.01	25.64	14.43	0.1985
600GUD	33.29	0.1982	35.05	33.70	17.21	0.1323
1250GUD	30.83	0.2469	42.72	29.79	13.33	0.1867
1215GTD	32.88	0.2670	42.13	45.39	21.65	0.2045
808GDD	30.95	0.3053	46.13	42.66	18.84	0.2465

3.2 Effect of Compaction Time

The thickness of the specimens during the successive compaction test was plotted in Fig. 5 (a). Increasing compaction time resulted in less thickness reduction in the initial 20 min, and then the thickness reduction tended to an equilibrium (defined as the thickness change less than 0.005 mm). This indicates that 20 min successive compaction at P=0.10 MPa before resin filling is enough for VIMP to achieve the desired part thickness. Fitting results show that the relationship between thickness and compaction time can also be simulated by the power law model:

$$h = h_{\mathrm{is}} - e \cdot t^{f} \tag{6}$$

Where h_{is} is the initial thickness under 0.10 MPa vacuum compaction pressure, t is the compaction time, e and f are the experimental parameters. The corresponding expression of the relationship between fiber volume fraction and the compaction time is:

$$V_{\mathrm{f}} = g \cdot t^{k} + V_{\mathrm{i}} \tag{7}$$

Where V_{i} is the initial fiber volume fraction under 0.10 MPa vacuum compaction pressure, g and k are the experimental parameters. Equation 7 fitting results are compared to the experimental data in Fig. 5(b), which shows a good agreement between them. Compared to the four sets of glass-fiber fabrics, the resulting thickness of carbon fiber fabric 300CUD has a large reduction in the initial 20 min. The parameters obtained are listed in Table 4.

3.3 Effect of Cyclic Compaction

Figure 6(a) shows that increasing number of cycles resulted in a decrease in thickness for the all fabrics. The thickness plotted in Fig. 6(a) was the minimum value during each cyclic compaction test. The thickness reduction reached equilibrium around 80 cycles for the all fabrics. A two-parameter power law model was established to fit the cyclic compaction thickness results. Fitting results show that the two-parameter power law model fits the cyclic compaction thickness data well, and the model can be defined as:

$$h = h_1 \cdot n_{\mathrm{c}}^{u} \tag{8}$$

Where h_1 is the minimum thickness in the first cyclic compaction test, n_{c} is the number of the cycles and u is the experimental parameter. And the corresponding relationship between the fiber volume fraction and the number of cycles can be expressed with the following model:

$$V_{\mathrm{f}} = V_1 \cdot n_{\mathrm{c}}^{m} \tag{9}$$

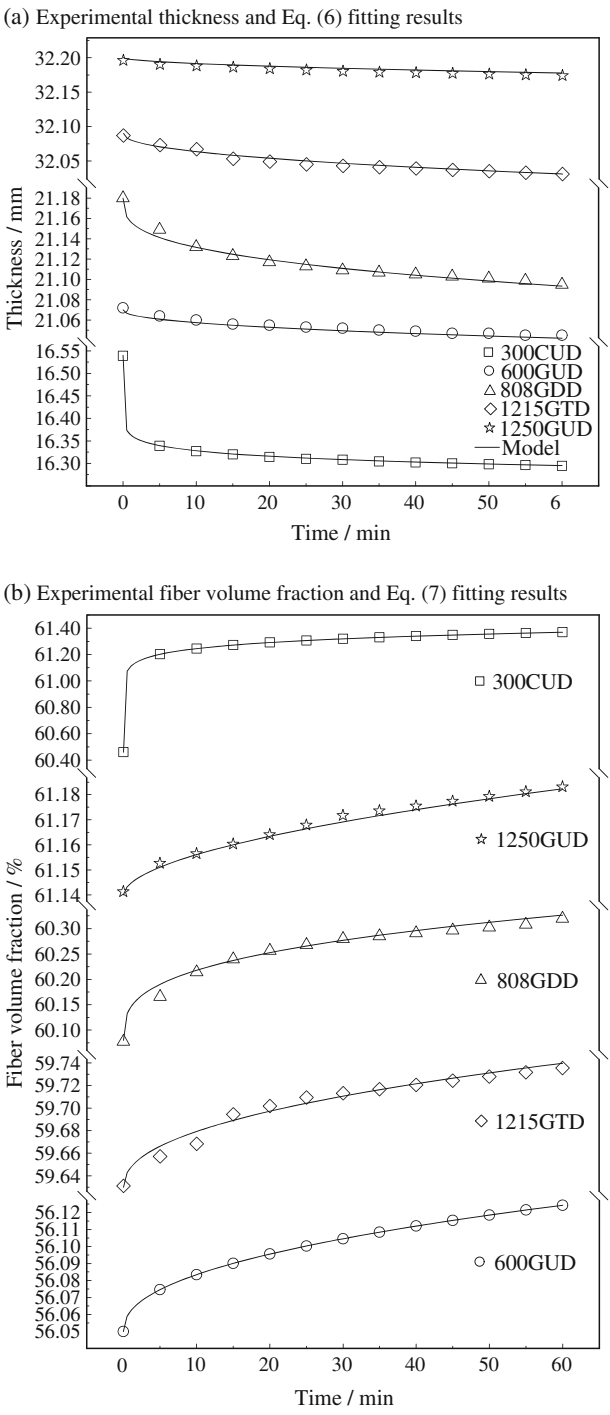

Fig. 5 Effect of compaction time on compaction behavior for five fabrics under 0.10 MPa vacuum pressure. **a** Experimental thickness and Eq. 6 fitting results, **b** Experimental fiber volume fraction and Eq. 7 fitting results

Table 4 Fitted parameters for compaction time models

Fabric	g	k	V_i/%	h_i/mm	e	f
300CUD	0.6506	0.08166	60.46	16.54	0.1761	0.08056
600GUD	0.01199	0.4456	56.05	21.07	0.004528	0.4440
1250GUD	0.06542	0.3240	60.08	21.18	0.02304	0.3232
1215GTD	0.01768	0.4458	59.63	32.09	0.009501	0.4458
808GDD	0.004642	0.5400	61.14	32.20	0.002501	0.5340

Where V_1 is the maximum value of fiber volume fraction in the first cyclic compaction test and m is the experimental parameter. Equation 9 fitting results are compared to the

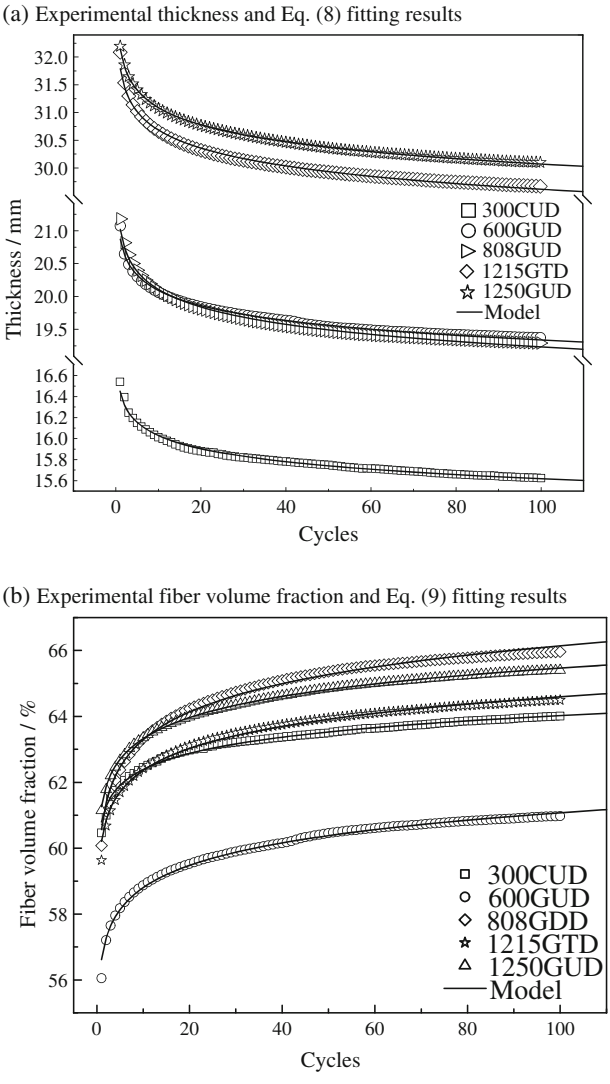

Fig. 6 Effect of cyclic compaction on thickness for five fabrics. **a** Experimental thickness and Eq. 8 fitting results, **b** Experimental fiber volume fraction and Eq. 9 fitting results

experimental data in Fig. 6(b), which shows a good agreement between the fitting results and the experimental data. The parameters obtained are listed in Table 5.

3.4 Effect of Number of Layers

The resulting fiber volume fraction and relaxation factor of the fabrics with different layer numbers under static compaction pressure 0.10 MPa at least 20 min were summarized in Table 6. As shown in Table 6, although the resulting fiber volume fraction increases as the layer numbers increase (i.e. it is easier to compact), there is less than 2.5% change in fiber volume fraction from 10 layers to 100 layers. It means that the effect of the number of layers on the fiber volume fraction of the dry preform in VIMP can be ignored. Therefore, the thickness of the dry preform in VIMP can be predicted by the conversion form of Eq. 1, as shown in Eq. 10:

$$h_{\mathrm{n}} = \frac{\rho_{\mathrm{a}} n}{\rho V_{\mathrm{A}}} \tag{10}$$

Where h_{n} is the thickness of n layer fabric preform and V_{A} is the average fiber volume fraction of different layer fabric preform. A good agreement between the experimental data and the predicted results was observed as shown in Fig. 7.

The resulting fiber volume fraction of 1250GUD is relatively higher than that of 600GUD, as shown in Table 6. It means that the resulting fiber volume fraction under compaction pressure is closely related to the weaving density. The higher weaving density means more easy to obtain high fiber volume fraction under the vacuum compaction pressure in VIMP. The resulting fiber volume fraction is relatively higher for the bi-axial and tri-axial knitted fabrics (808GDD and 1215GTD) than for the unidirectional fabric 600GUD. Although the bi-axial and tri-axial weaving methods have less chance than the unidirectional fabric for compaction nesting, the weaving density of 808GDD and 1215GTD are higher than that of 600GUD. The fiber volume fraction of 300CUD is also higher than that of 600GUD, which means the compaction behavior is closely related with the fiber type.

Table 6 also shows that increasing number of layers resulted in less relaxation factor increase (i.e. it is easier to relax), and there is obvious difference among different fabrics. Although the resulting fiber volume fraction increases with the relaxation factor for the same fabric, there is no corresponding tendency for the various fabrics.

3.5 Variation of Part Thickness During Infusion Process

The thickness and fiber volume fraction of the fabric preform during pre-filling stage depend on the dry fabric compaction behavior as mentioned in Sections 3.1, 3.2, 3.3, 3.4.

Table 5 Fitted parameters for cyclic compaction models

Fabric	h_1/mm	u	m	V_1/%
300CUD	16.45	−0.01127	0.01122	60.8
600GUD	20.87	−0.01655	0.01644	56.62
1250GUD	21.02	−0.01929	0.01911	60.57
1215GTD	31.79	−0.01538	0.01526	60.21
808GDD	32.14	−0.01445	0.01442	61.26

Table 6 Fiber volume fraction and Relaxation factor for various fabrics

Number of layers	Fiber volume fraction (%)/relaxation factor				
	300CUD	600GUD	808GDD	1215GTD	1250GUD
10	60.08/0.3508	57.03/0.3856	62.39/0.3153	59.24/0.2882	61.08/0.2532
20	60.15/0.3515	57.05/0.3858	62.40/0.3155	59.81/0.2950	61.87/0.2540
40	60.67/0.3571	57.05/0.3859	62.41/0.3156	59.83/0.2952	61.89/0.2542
60	61.27/0.3634	57.79/0.3937	62.44/0.3159	61.14/0.3103	62.07/0.2564
80	61.55/0.3663	58.08/0.3966	62.47/0.3162	61.37/0.3129	62.17/0.2576
100	61.82/0.3691	58.19/0.3978	62.48/0.3164	61.53/0.3147	62.71/0.2639

During the filling stage, within the saturated region, the total compaction pressure applied to the cavity is both partly carried by the fluid and partly carried by the preform. This balance of atmospheric pressure by the fluid pressure and the preform compaction stress was expressed by Correia in [11]. The saturated part of the reinforcement is thus subjected to a wet unloading. As the local fluid pressure increases, the compaction stress on the reinforcement decreases, and the local fiber volume fraction decreases. During the post-filling, the fluid pressure decreases as the excess resin is drawn out of the mold cavity. Therefore the preform compaction stress increases and the reinforcement is subjected to wet compaction. Note that during these three phases (dry compaction, wet unloading and wet compaction) the permeability, porosity and thickness of the preform dynamically change with the varying preform deformation because of compaction pressure variation [3].

Thickness variation during filling and post-filling process is a manifestation of the coupled fabric compaction and resin flow. To achieve a desired thickness in the final product, vacuum infusion experiments are done to investigate the actual thickness variation characterization of the fabric preform. Considering the actual process conditions, the actual thickness variation of the following three cases were investigated in this paper. In the three cases, the same fabric configuration (ten layers of 1250GUD fabrics, one layer of peel-ply and one layer of distribution medium) is used in the characterization experiments, except that the in-plane dimensions are 60 cm by 15 cm. The micrometer gauges are located on the

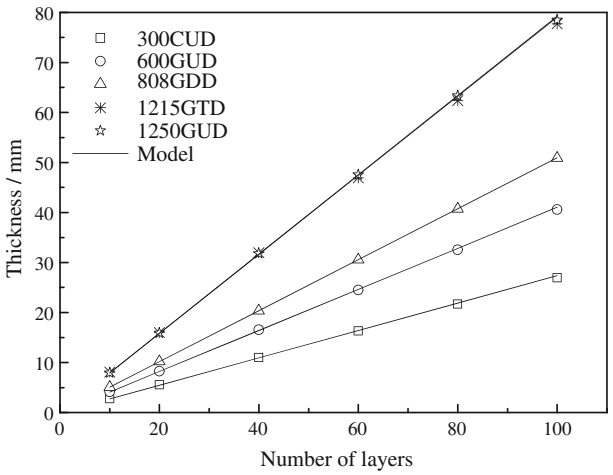

Fig. 7 Experimental thickness and average thickness predicted from Eq. 10 for VIMP

point 20 cm away from the injection line. The fabric configuration and the experimental setup are shown in Fig. 8.

The experimental setup is prepared as follows. The fabric preform is placed on the solid plate mold. The preform is covered with a peel-ply, and the peel-ply is covered by a layer of distribution medium. Spiral tubes are used at the injection gate and ventilation port. A vacuum bag is placed to cover them, and they are sealed using tacky tape sealant. Since the surface of the fabric is irregular, small lightweight square plate is placed under the tips of dial gauges to measure an averaged thickness at gauge locations. Vacuum is applied for 20 min to minimize air between fibers and to achieve almost steady compaction. The data acquisition is started with the vacuum, and it is continued even after gelation to see the shrinkage during curing stage. The difference among three cases is as follows.

In case 1, vacuum vent is covered by a layer of semi-membrane. The semi-membrane is permeable for gases and impermeable to selected resins [4]. It means that air and volatiles can be continuously evacuated from the preform through the vacuum vent, but the resin cannot bleed out. After the injection is complete, the injection line is closed immediately. Vacuum is still provided through the semi-membrane, but as the resin cannot penetrate it, resin pressure will stabilize to the inlet pressure.

In case 2, both the injection line and vacuum vent are closed immediately after the filling is complete. The resin cannot flow into the preform and bleed out through the vent. The resin pressure will stabilize and redistribute in the preform spontaneously.

In Case 3, the injection line is closed immediately after the injection is complete. Vacuum is still provided, and the resin can bleed through the opened vacuum vent. The resin pressure will stabilize and redistribute with the resin bleeding until the resin curing.

Figure 9 shows that the thickness varies with time during pre-filling, filling and post-filling stage in the infusion experiments for the three cases. The thickness of the fabric preform is almost steady before filling. As shown by a star in Fig. 9, there is a less increase in preform thickness at the beginning of the filling stage, because a little of gas will get into the mold cavity when the resin inlet is opened. When the resin wets a region of the preform near the flow front, the thickness decreases right away due to the lubrication effect as shown by a delta in Fig. 9, also as observed in Tackitt et al. [10]. The lubrication effect helps the fibers to stack more effectively, and this effect is very significant for the uni-axial and dual-axial fabrics used in the wind turbine blade industry. After the flow front passed, the thickness in the wet region increases quickly due to the decrease of the compaction stress (Further propagation of the flow front results in an increase in the local resin pressure as observed in Yenilmez [5], and hence a decrease in the compaction pressure.). The thickness continues to increase until a maximum value (as shown by a circle in Fig. 9) during the post-filling stage, and then it begins to decrease. The resin flow continues after the filling phase is completed as it does take certain time for the pressure field to become uniform. Thus, even after the inlet is closed, the resin within the part is not in equilibrium, as its pressure is non-uniform and within the elastic

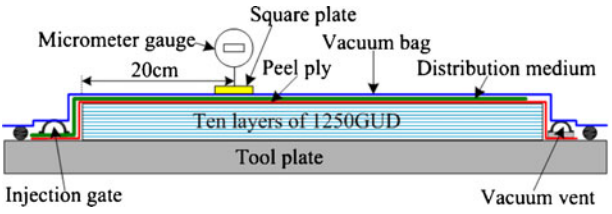

Fig. 8 Fabric configuration and experimental setup for infusion experiment

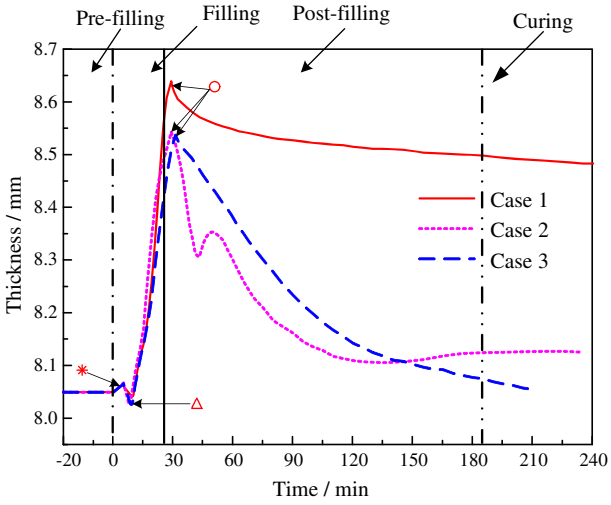

Fig. 9 Part thicknesses measured by micrometer gauges during the pre-filling, filling and post-filling stages of infusion experiments in which ten layers of 1250GUD were used

fiber bed it cannot drop to vent pressure instantaneously. As the resin pressure drops, the compacting load on the preform increases and the preform will compact further squeezing the resin out. If the final resin pressure will reach a constant value before the resin gelation, the thickness should be uniform at the end.

In case 1, the vent is covered by a layer of semi-membrane, the resin cannot bleed out and it will be redistribution in the part to achieve equilibrium. And a certain level of vacuum can be maintained after the preform is filled. This will compact the part and lead to more uniform thickness. In case 2, vacuum vent is closed by shutting off the connected tube between vent and vacuum pump. Although the resin cannot bleed out, the connected tube at the vent side will gather some resin. That is another way of loss of resin. The loss of resin results in more decrease of thickness in the part for case 2. In case 3, the vacuum vent remains open and the resin can bleed through the vent. And a certain level of vacuum can be maintained after the preform is filled. Compared to the three cases, the thinnest thickness

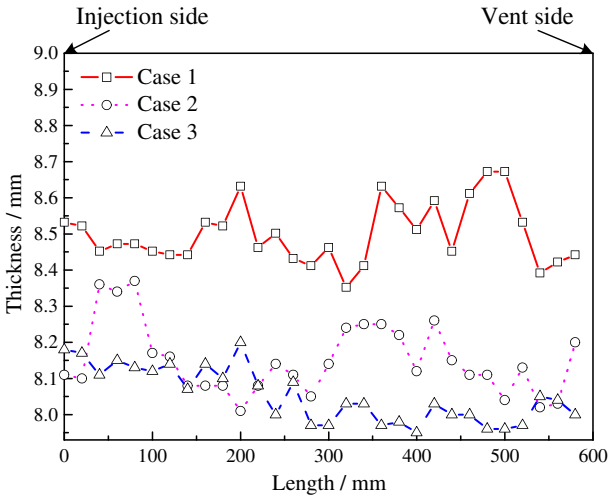

Fig. 10 Final part thickness distribution along the length direction for the different three cases

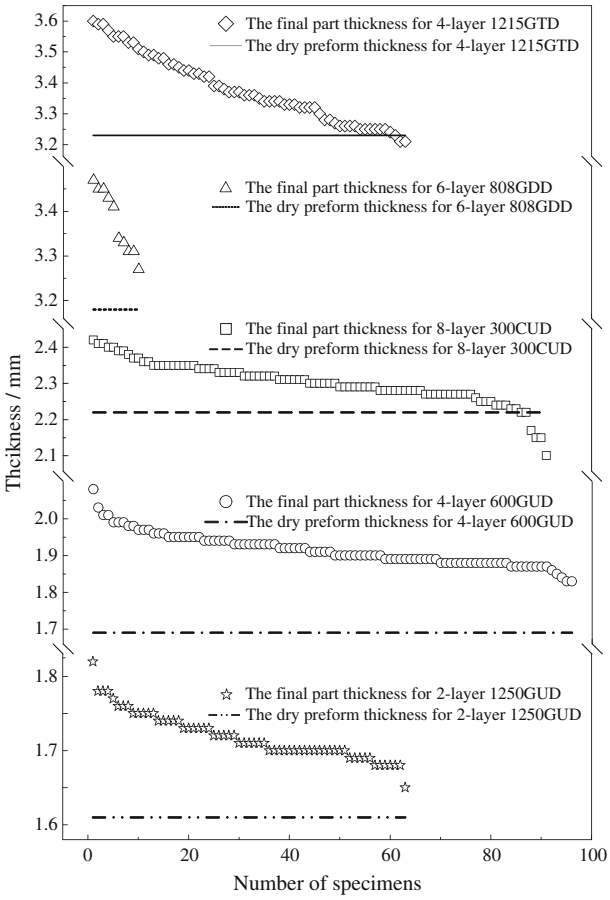

Fig. 11 Comparison of the final thickness and the dry preform thickness for various fabrics

can be gotten in case 3 as shown in Fig. 9. That is, resin bleeding for extended time periods after the filling is a way to reducing the variability in part thickness for VIMP.

Next into the curing stage, the curing shrinkage of resin will result in less thickness reduction as shown in Fig. 9.

Table 7 Thickness and fiber volume fraction for the dry prefom and the final part

Fabrics	Layers	The dry preform		$\frac{h_F-h_P}{h_P} \times 100\%$	The final part		$\frac{V_F-V_P}{V_P} \times 100\%$
		h_P/mm	V_P/%		h_F/mm	V_F/%	
300CUD	8	2.22	60.06	3.60	2.30	57.97	−3.48
600GUD	4	1.69	55.91	13.60	1.92	50.21	−10.19
808GDD	6	3.18	60.02	6.28	3.38	56.47	−5.91
1215GTD	4	3.23	59.24	4.64	3.38	56.61	−4.44
1250GUD	2	1.61	61.13	6.83	1.72	57.22	−6.40

V_P and V_F stand for the fiber volume fraction of the dry preform and the final part, respectively. h_P and h_F stand for the thickness of the dry fabric preform and the final part, respectively

3.6 The Final Part Thickness

The final part thickness distribution along the length direction (from the injection line to the vacuum vent) for the three cases as shown in Fig. 10. The average final part thickness in case 1 is about 0.30 mm thicker than that in case 2, and the thinnest part thickness is obtained in the case 3. It is consistent with the previous results in Fig. 9. As shown in Fig. 10, the final part thickness is not uniform distribution in length direction from the injection side to the vent side, and there is no obvious trend in thickness variation.

Figure 11 shows that the final part thickness is thicker than the dry preform thickness for the all fabrics. The statistical results are summarized in Table 7. The fiber volume fraction difference between the final part and the dry preform is 2%~5.7% for the five kinds of fabrics. Statistical results show that the final part thickness is equivalent to the thickness of the dry preform under the 0.08 MPa vacuum compaction pressure in VIMP.

4 Conclusions

The step compaction results indicate that as the vacuum pressure increases, the fiber volume fraction of the dry preform increases following a three-parameter power law model. And the thickness decreases following the corresponding the power law model.

The successive compaction results show that increasing compaction time resulted in less thickness reduction in the initial 20 min, and then the thickness reduction tended to equilibrium. The relationship between the fiber volume fraction and the compaction time, between the thickness and the compaction time can be expressed by the power law models.

The cyclic compaction results show that increasing number of cycles resulted in a decrease in thickness for the all fabrics. Thickness reduction reached equilibrium around 80 cycles in cyclic compaction tests. The relationship between thickness and cycles can be expressed by a two-parameter power law model. And the relationship between fiber volume fraction and cycles can be expressed by the corresponding model.

As the number of layers increases, the relaxation factor and fiber volume fraction increase. This can be attributed to yarn flattening, increased yarn packing fraction, and increased nesting between layers when the spacing between yarns is large. Although the resulting fiber volume fraction increases as the layer numbers increase, there is less than 2.5% change in fiber volume fraction from 10 layers to 100 layers.

The part thickness varies as a function of spatial coordinates and time during pre-filling, filling and post-filling stages in VIMP. During the pre-filling stage, the thickness of the fabric preform depends on the dry fabric compaction behavior. During the filling stage, the thickness decreases due to the lubrication effect can be observed in the flow front. Once the flow front passed, the thickness increases quickly until a maximum value during the post-filling stage, and then it begins to decrease until curing. Processing parameters such as semi-membrane and vent open time will significantly affect the thickness variation rules.

The final part thickness is significantly affected by the processing parameters in VIMP. Statistical results show that the final part thickness is equivalent to that of the dry preform under the 0.08 MPa vacuum compaction pressure in VIMP. The fiber volume fraction difference between the final part and the dry preform is 2%~5.7% for the five kinds of fabrics.

Acknowledgement This work is fund by the national “863” plan project of China (2007AA03Z563) and the science & technology project of Hunan Province (2009FJ1002). The authors would like to acknowledge the support of the Cooperative Zhuzhou Times New Material Technology Co., Ltd for this work.

References

1. Bayldon, J.M., Daniel, I.M.: Flow modeling of the VARTM process including progressive satuation effects. Compos. Part A: Appl. Sci. Manufact. **40**, 1044–1052 (2009)
2. Yuexin, D., Zhaoyuan, T., Yan, Z., Jing, S.: Compression responses of preform in vacuum infusion process. Chin. J. Aeronaut. **21**, 370–377 (2008)
3. Govignon, Q., Bickerton, S., Kelly, P.A.: Simulation of the reinforcement compaction and resin flow during the complete resin infusion process. Compos. Part A: Appl. Sci. Manufact. **41**, 45–57 (2010)
4. Simacek, P., Heider, D., Gillespie Jr., J.W., Advani, S.: Post-filling flow in vacuum assisted resin transfer molding process: Theoretical analysis. Compos. Part A: Appl. Sci. Manufact. **40**, 913–924 (2009)
5. Yenilmez, B., Senan, M., Sozer, E.M.: Variation of part thickness and compaction pressure in vacuum infusion process. Compos. Sci. Technol. **69**, 1710–1719 (2009)
6. Kelly, P.A., Umerb, R., Bickerton, S.: Viscoelastic response of dry and wet fibrous materials during infusion processes. Compos. Part A: Appl. Sci. Manuf. **27**, 868–873 (2006)
7. Hammami, A.: Effect of reinforcement structure on compaction behavior in the vacuum infusion process. Polym. Compos. **22**, 337–348 (2001)
8. Luo, Y., Verposet, I.: Compressibility and relaxation of a new sandwich textile preform for liquid composite molding. Polym. Compos. **20**, 179–191 (1999)
9. Robitaille, F., Gauvin, R.: Compaction of textile reinforcements for composites manufacturing: I-review of experimental results. Polym. Compos. **19**, 543–600 (1998)
10. Tackitt, K.D., Walsh, S.M.: Experimental study of thickness gradient formation in the VI process. Mater. Manuf. Process. **20**, 607–627 (2005)
11. Correia, N.C., Robitaille, F., Long, A.C., Rudd, C.D., Simacek, P., Advani, S.G.: Analysis of the vacuum infusion molding process: I. Analytical formulation. Compos. Part A: Appl. Sci. Manufact. **26**, 1645–1656 (2005)
12. Robitaille, F., Gauvin, R.: Compaction of textile reinforcements for composites manufacturing. II: Compaction and relaxation of dry and H_2O-saturated woven reinforcements. Polym. Compos. **19**, 543–557 (1998)
13. Kruckenberg, T., Ye, L., Paton, R.: Static and vibration compaction and microstructure analysis on plain-woven textile fabrics. Compos. Part A: Appl. Sci. Manufact. **39**, 488–502 (2008)